Available online at www.sciencedirect.com

ScienceDirect

Procedia Engineering 13 (2011) 133–140

Engineering Procedia

5th Asia-Pacific Congress on Sports Technology (APCST)

Prediction of passive and active drag in swimming

Angus Webb*, Joseph Banks, Christopher Phillips, Dominic Hudson, Dominic Taunton, Stephen Turnock

University of Southampton, University Road, Southampton, SO17 1BJ, United Kingdom

Received 28 March 2011; revised 14 May 2011; accepted 15 May 2011

Abstract

In order to understand the physical origin of passive resistance in swimming the resistance breakdown for a swimmer is investigated. A combination of empirical methods and theoretical analysis is used to predict passive resistance in the speed range 0 – 2 ms^{-1} and is shown to provide similar results to those from experimental testing. Typical magnitudes of wave, viscous pressure and skin friction resistance contribute 59%, 33% and 8% of total passive resistance respectively at free swim speed. A comparison is made between the widely used Velocity Perturbation Method and a Naval Architecture based approach in predicting active drag. For the swimmer investigated the two approaches predict active drag of 131.4 N and 133.9 N for a swimming speed of 1.53 ms^{-1}. However, the results predicted from the Velocity Perturbation Method have a much higher uncertainty and the Naval Architecture based approach is suggested as a more robust method of predicting active drag.

Selection and peer-review under responsibility of RMIT University

Keywords: Swimming; passive drag; active drag

1. Introduction

Active drag is commonly used as a single value that represents a swimmer's performance. Active drag may be viewed as a composite quantity that includes both the resistive drag of the swimmer and the propulsive thrust generated for a given speed and stroke rate. Typically, this value is found from a time average over the duration of an integer number of stroke cycles. Various techniques have been used to measure active drag, however the results from these studies appear to differ [1]. The aim of this study is

* Corresponding author. Tel.: +44 (0) 23 8059 6625; fax: +44 (0) 2380 597744.
E-mail address: angus.webb@soton.ac.uk.

1877–7058
doi:10.1016/j.proeng.2011.05.063

to identify the limitations of current active drag prediction techniques and to suggest a new method with less sensitivity to experimental error.

The over-speed velocity perturbation method is investigated in this paper, as it is considered to provide the most representative conditions for natural swimming [2]. Naval architecture based methods are used to aid in the understanding of active drag [3], and a resistance breakdown of an object moving on the free surface is detailed, identifying wave making drag and viscous pressure drag as the main contributors. To conduct the velocity perturbation method, a tow device was used that allows swimmers to be towed over a speed range of 0 – 3 ms^{-1} and the net tow force measured for either passive or active swimming. The measurement of active drag requires multiple tests to be conducted at a range of speeds, with the primary assumption that the swimmer will deliver equal power for each test.

A naval architecture based approach for predicting active drag is proposed that requires the measurement or *ab-initio* prediction of passive drag. Passive drag results are compared with those published in literature, identifying differences due to the body shape tested for passive drag. The active drag prediction from the naval architecture based approach is compared with the prediction from the velocity perturbation method. The uncertainty of each method is analysed, identifying the velocity perturbation method to be more sensitive to errors in the experimental measurements.

2. Methodology

2.1. Components of resistance for passive drag

The passive drag of a swimmer is the resistance generated by the non-propulsive parts of the swimmer's body. This is assumed to be the whole body, not including the arms below the shoulders. To accurately predict the passive drag of a swimmer, it is necessary to understand how the total resistance is divided into individual components. Figure 1 indicates the contribution of pressure and viscous resistance, where pressure resistance consists of wave and viscous pressure components. The latter is due to regions of separated flow and interaction between the wave field and boundary layer development. The frictional component is due to the surface shear stress over the wetted area of the swimmer.

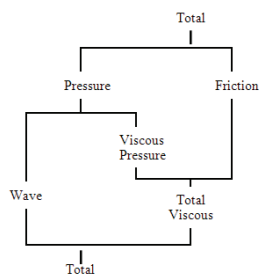

Fig. 1. Components of resistance for an object moving at a constant velocity on the free surface [3].

The component contribution to the total resistance is given as.

$$R_{Total} = R_{Wave} + R_{Viscous\,\mathrm{Pr}essure} + R_{Frictional} \quad (1)$$

The wave resistance component is predicted using an in-house software code for potential flow based thin ship theory [4]. This requires a basic geometry, from which an array of source strengths distributed along the body centre plane is generated to model the wave disturbance generated by the swimmer. The

wave resistance was determined for the speed range 0 – 2 ms^{-1}. Figure 2 shows the wave resistance coefficient against a length-based Froude number for a swimmer of height 1.79 m. It can be seen that for Froude numbers less that 0.18, the resistance prediction varies considerably. The requirement for more harmonics to represent the wave system at low Froude numbers leads to this inaccuracy. Disregarding these large peaks for Froude numbers less than 0.18, the resistance hump appears to occur at a Froude number of 0.23. The wave resistance hump is caused by wave interference along the body. Constructive interference causes the resistance humps and destructive interference causes the resistance hollows. Figure 3 displays the wave profile prediction from Thin Ship Theory for a free swim speed of 1.55 ms^{-1}.

Wave resistance is calculated as,

$$R_{Wave} = 0.5\rho V^2 A_{Wetted} C_W, \tag{2}$$

where ρ is the density of the fluid, V is the velocity of the body and A_{Wetted} is the wetted surface area of the body, which was determined using,

$$A_{Wetted} = 0.20247 H^{0.725} W^{0.425} \tag{3}$$

with H the height (m) and W weight (kg) [5]. The skin friction coefficient was determined from the ITTC 1957 correlation line for turbulent flow [3],

$$C_f = \frac{0.075}{\left(\log(\mathrm{Re}) - 2\right)^2} \tag{4}$$

where Re is the Reynolds number of the body. The skin friction resistance is calculated using,

$$R_{Frictional} = 0.5\rho V^2 A_{Wetted} C_f. \tag{5}$$

Viscous pressure resistance was assumed to be due to bluff body separation, with viscous pressure resistance due to boundary layer growth negligible. A pressure drag coefficient C_{Dp} for an elliptical bluff body of 0.3 was chosen [6]. The viscous pressure resistance is calculated as;

$$R_{Viscous\,\mathrm{Pressure}} = 0.5\rho V^2 A_{prjected} C_{Dp} \tag{6}$$

where $A_{Projected}$ is the projected area, determined from a photograph of the swimmer.

Figure 4 shows the prediction of total resistance against velocity. At the free swim speed of 1.55 ms^{-1} wave making resistance, viscous pressure resistance and skin friction resistance contribute to 59%, 33% and 8% of the total resistance respectively. This agrees with findings published on an experimental study, investigating the wave resistance of a swimmer [7]. Also included in figure 4 are experimental data for the same swimmer. It may be observed that this relatively crude prediction of total passive resistance is reasonably accurate, particularly around the free swim velocity. The prediction of resistance is sensitive to the choice of pressure drag coefficient. There will also be measurement uncertainty for the experimental data, which is not considered here.

In order to compare passive drag data with that of other swimmers at different velocities it is necessary to express it as a total passive drag coefficient. The total passive drag coefficient was determined using Equation 7, which is the standard naval architecture approach [3],

$$C_{Total} = \frac{R_{Total}}{0.5\rho V^2 A_{Wetted}}. \tag{7}$$

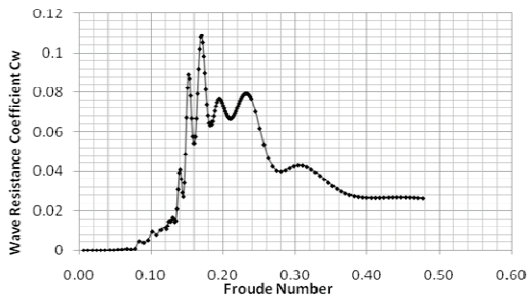

Fig. 2. Wave resistance coefficient against non-dimensional length based Froude number.

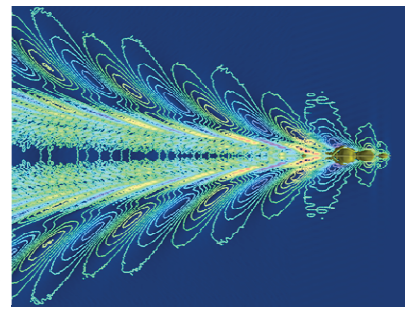

Fig. 3. Thin Ship Theory wave pattern prediction for free swim speed of 1.55 m/s showing contours of surface elevation. The swimmer is moving left-to right.

2.2. Prediction of active drag

2.2.1. Velocity perturbation method (VPM)

Prediction of active drag using the velocity perturbation method [8] requires a swimmer to be tested at two different velocities, a free swim velocity and a perturbed velocity. The perturbed velocity is achieved by exerting an additional known resistance on the swimmer, which can be achieved through a variety of methods. The original method [8] requires the swimmer to tow an object of known resistance, resulting in a decrease in velocity. In an alternative approach [2] the active swimmer is towed at an increased speed with the residual resistance measured using a dynamometer.

The theory of the VPM does not change whether the perturbed velocity is achieved by over speeding or under speeding the swimmer. Mason *et al.* [2] proposes that over speeding the swimmer by 10% of their free swim speed provides enough speed to ensure the towline remains tight but does not have a significant impact on stroke dynamics.

It is assumed the swimmer produces equal power for the free swim and the swim at the perturbed velocity. To ensure equal effort for both conditions the swimmer is tested at maximal effort, with enough recovery time between tests to ensure no fatigue [8].

Active drag at the free swim velocity may be expressed,

$$R_{Freeswim} = \frac{1}{2}\rho V_{Freeswim}{}^2 A C_d \tag{8}$$

where ρ is the density of the fluid, V is the free swim velocity, A is the wetted surface area and C_d is the drag coefficient.

The resistance of the swimmer at the perturbed velocity may be expressed,

$$R_{Perturbed} = \frac{1}{2}\rho V_{Perturbed}{}^2 A C_d \tag{9}$$

For the free swim and perturbed velocities, C_d and A are assumed to remain constant and the resistance of the swimmer is proportional to the square of velocity. Therefore the resultant force acting on the swimmer in the perturbed velocity condition is, $R_{Perturbed} - R_{Towline}$, where $R_{Towline}$ is the force measured by the dynamometer.

With the assumption of constant effort for both the free swim and in the perturbed velocity condition,

$$R_{Freeswim} \cdot V_{Freeswim} = \left(R_{Perturbed} - R_{Towline}\right) \cdot V_{Perturbed} \quad (10)$$

Substituting Equations 8 and 9, and rearranging provides the expression for active drag as,

$$R_{Freeswim} = \frac{R_{Towline} \cdot V_{Perturbed} \cdot V_{Freeswim}^{\ 2}}{V_{Perturbed}^{\ 3} - V_{Freeswim}^{\ 3}} \quad (11)$$

2.2.2. Naval Architecture Based Approach (NABA)

The naval architecture based approach NABA is based on the analysis of a model scale self-propulsion experiment for ships [3]. The purpose of a self-propulsion experiment is to determine the interaction effects between the propeller and the naked hull. Before conducting a self-propulsion experiment, it is necessary to test the hull and the propeller separately. This determines the naked hull resistance as a function of V for the hull, and K_T, K_Q as a function of J for the propeller, where K_T is a non-dimensional thrust coefficient, K_Q a non-dimensional torque coefficient and J the advance ratio, equal to V/nD, where V is the advance velocity, n the revolutions per second and D is the diameter of the propeller. When testing the hull and the propeller together, the accelerated flow over the hull due to the propeller causes the hull to have greater resistance and the wake produced by the hull causes the propeller to have a smaller advance velocity.

When conducting a model self-propulsion experiment, a model fitted with a propeller and motor is towed from a dynamometer at a fixed velocity. The propeller n is set and the tow force measured is R-T where R is the hull resistance and T is the thrust produced by the propeller. Usually the propeller n is varied until R-T is zero; this is called the self-propulsion point. By comparing the velocity and thrust measured at the self-propulsion point with data for the individual hull and propeller experiments, the interaction effects may be determined. One of the key interaction parameters is the thrust deduction *(1-t)*, which describes the additional thrust above the naked hull resistance required to propel the hull at that velocity, due to the increased resistance from the flow generated by the propeller. More detail on ship self-propulsion experiments may be found in Molland *et al*. [3].

To apply this theory to swimming it may be assumed that the arms act as the propeller and the remaining body as the hull. This study does not attempt to determine K_T and K_Q for the arms, however J is considered an important parameter when setting stroke rate. The naked hull resistance can either be determined from a passive drag experiment or predicted as shown in Section 2.1.

Unlike a model ship self-propulsion experiment, the self-propulsion velocity of the swimmer is already known, however the thrust is not and cannot be measured at the free swim velocity. Therefore, it is necessary to test the swimmer at a different velocity and measure the tension in the towline, R-T. In this study, the swimmer was towed 5%, 10% and 15% faster than their free swim velocity. To ensure the efficiency of the propulsion does not change between the free swim condition and the towed conditions it is necessary to maintain the same advance ratio J. Therefore, when increasing the speed, the swimming stroke rate needs to be increased accordingly. It is assumed the stroke is a perfect six beat front crawl and by adjusting the arm stroke rate, the leg stroke rate follows. It is assumed there is constant power between

the free swim conditions and all of the towed conditions. With a constant *J*, this translates to constant non-dimensional thrust for all conditions.

For each test, the mean stroke *R-T* was measured. Since the swimmer is being towed faster than their free swim speed, it is necessary to correct their naked hull resistance back to that for the free swim velocity using a correction value $\Delta R_{Correction}$. This value is the difference between the passive drag resistance at the tow speed and the passive drag at the free swim speed. In this study, the predicted resistance data are used to estimate the correction value and the naked resistance. A key difference is that for the NABA resistance is not assumed to scale as V^2.

As a result, the active drag may be determined as,

$$R_{Active} = \left(R - T\right)_{Measured} - \Delta R_{Correction} + R_{Naked} \quad (12)$$

The thrust deduction may be determined by,

$$\left(1 - t\right) = \frac{R_{Naked}}{R_{Active}} \quad (13)$$

which describes the additional resistance of the body due to the flow generated by the arms. It may also be used as a value to describe the effectiveness of the propulsion.

2.3. Experimental setup

The free-swimming speed was determined by timing the swimmer over a 15m section of a 25m pool. A purpose-built tow system with a speed range of 0 – 3 ms^{-1} was used to tow the swimmer at a fixed speed. The swimmer is towed using a waist harness, which allows them to adjust their body position and has minimal impact on their stroke. The resistance generated by the swimmer is measured using three force blocks on which the system is mounted. Force and speed are measured as linearly varying analogue signals, which are converted using a 16-bit analogue to digital converter. Figure 5 displays typical data gathered during a test run. The acceleration phase at the beginning can be seen as the large peak in recorded force. The mean *R-T* value is measured during a constant velocity phase and to ensure repeatability between results, an integer number of peaks were taken for the mean.

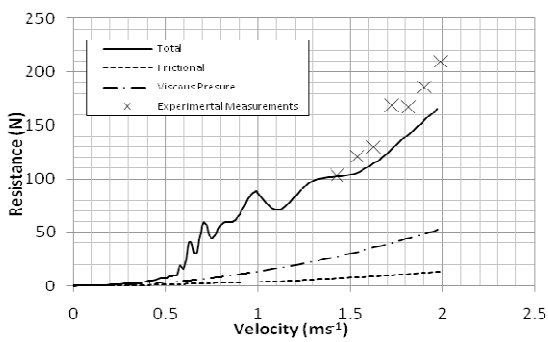

Fig. 4. Total, viscous pressure and skin friction resistance against velocity for a swimmer with arms by side, clearly displaying humps and hollows from wave interference. Experimental data can be seen to correlate well with predicted total resistance.

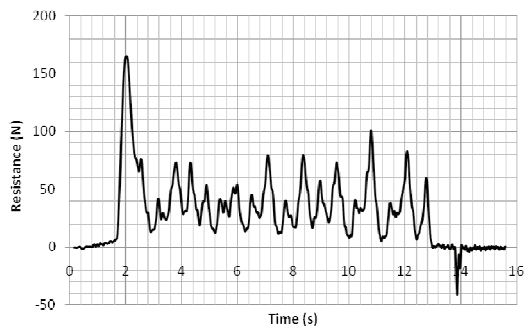

Fig. 5. Typical run trace, clearly displaying the acceleration phase at the beginning and the stroke cycles during the constant velocity phase.

3. Results and Discussion

Table 1 presents the test conditions used to calculate active drag from both the NABA and the VPM. The passive drag coefficient from Kolmogorov's Table 2 [8] was found as 0.025. This value is significantly smaller than the mean passive drag coefficient in Table 1. Kolmogorov investigated swimmers in the 'front gliding position' whereas this study investigated swimmers with arms at the side as it is thought this better represents the non-propulsive body shape. It is also unclear as to whether swimmers were tested on the free surface by Kolmogorov.

Table 1. Passive and active drag prediction results using the NABA and VPM.

Test Condition	No. Runs	Speed (m/s)	Passive R (N)	Passive Ct	Resistance Correction (N)	R-T (N)	Active Drag NABA (N)	(1-t) NABA	Active Drag VPM (N)	(1-t) VPM	J
Free Swim	2	1.53 ± 0.03	104.05	-	-	-	-	-	-	-	2.85 ± 0.06
5% Over speed	6	1.69 ± 0.028	119.30	0.04526	15.25	41.97 ± 4.13	130.78 ± 2.96	0.80	131.95 ± 15.22	0.79	2.98 ± 0.11
10% Over speed	4	1.73 ± 0.017	124.25	0.04521	20.19	49.18 ± 1.79	133.04 ± 1.49	0.78	126.66 ± 7.64	0.82	2.98 ± 0.07
15% Over speed	2	1.74 ± 0.002	125.99	0.04520	21.93	55.75 ± 1.91	137.87 ± 2.28	0.75	135.44 ± 6.03	0.77	3.18 ± 0.03
Mean				0.04522			133.90	0.78	131.35	0.79	
Standard Deviation				0.000034			3.62	0.021	4.42	0.03	

Comparing the active drag predictions from the NABA and the VPM in Table 1, it can be seen both methods produce similar results, with the standard deviation of the NABA less than the VPM. The uncertainty values displayed in Table 1 were determined from the standard deviation over the number of runs completed. By comparing the uncertainty of the individual values for the NABA and the VPM, it can be seen the uncertainty is much greater for the VPM. The largest uncertainty experienced is for the 5% over speed test, which may be due to the uncertainty in the J value for this case, which is greater than that of the other conditions. This perhaps identifies the importance of stroke rate on the accuracy of predicting active drag with the VPM.

There appears to be an increasing trend in the NABA prediction of active drag with tow velocity. Each tow velocity should provide the same active drag value, if the correct resistance correction is applied and the efficiency of the propulsor remains the same. This trend may be due to an error in the stroke rate, where changing the required stroke rate may have only resulted in the out of water phase being adjusted with the arm velocity through the water remaining the same. In addition, post analysis of the stroke rate found the swimmer failed to achieve the required stroke rate and as a result, the J value did not remain constant.

By comparing Equations 11 and 12, it can be seen that the sensitivity of the active drag prediction to the measured *R-T* value is greater for the VPM. This may explain the larger uncertainty for the VPM predictions in Table 1 and hence the NABA may be more robust in predicting active drag.

Error in the *R-T* value may be caused by non-equal effort, or changes in stroke technique, between towed and free swim conditions. This error may be reduced by ensuring the swimmer is appropriately acclimatised under testing conditions before *R-T* measurements are taken.

4. Conclusion

A study of the resistance breakdown of a swimmer has been conducted. This has allowed a reasonably accurate prediction of passive drag assuming the total resistance is made up of wave resistance, pressure resistance and skin friction resistance. The passive drag prediction is seen to produce similar results to drag measurements taken from passively testing a swimmer.

The Velocity Perturbation Method and a proposed Naval Architecture based approach are investigated and used to predict active drag. Both methods produce similar results, however the uncertainty for the VPM is much greater. Error in the active drag prediction may be caused by testing at the wrong stroke rate and through inconsistency in the effort from the swimmer. It is suggested the stroke rate should be adjusted to maintain a constant advance ratio, J, when over speed testing. It is believed the naval architecture based approach provides a more robust prediction of active drag since it is less sensitive to experimental error.

References

[1] Toussaint, H. M., Roos, P. E., Kolmogorov, S., The determination of drag in front crawl swimming. *Journal of Biomechanics* 2004, 1655 – 1663.

[2] Mason, B., Alcock, A., Biomechanical Analysis of Active Drag in Swimming. *XXV ISBS Symposium* 2007, Ouro Preto, Brazil, 212 – 215.

[3] Molland, A. F., Turnock, S.R., Hudson, D.A. (2011) *Ship Resistance and Propulsion: Practical Estimation of Ship Propulsive Power*, Cambridge University Press.

[4] Mitchell, J. H., The Wave Resistance of a Ship. *Philosophical Magazine and Journal of Science* 1898, Vol: 5 – 45.

[5] DuBois D; DuBois EF: A formula to estimate the approximate surface area if height and weight be known. *Arch Int Med* 1916 17:863-71.

[6] Hoerner, S.F. *Fluid-Dynamic Drag: Theoretical, Experimental and Statistical Information*, Hoerner Fluid Dynamics, Bakersfield, CA, 1965.

[7] Vennell, R., Pease, D., Wilson, B., Wave drag on human swimmers. *Journal of Biomechanics* 2006, 39, 664 – 671

[8] Kolmogorov, S. V., Duplishceva, O. A., Active Drag, Useful Mechanical Power Output and Hydrodynamic Force Coefficient in Different Swimming Strokes at Maximal Velocity. *Journal of Biomechanics* 1992, Vol. 25, No.3, 311 – 318.